CDF/PUB/EXOTIC/PUBLIC/9775

Search for the Supersymmetric Partner of the Top Quark in Dilepton Events Produced in $p\bar{p}$ Collisions at $\sqrt{s}$ =1.96 TeV

The CDF Collaboration

URL http://www-cdf.fnal.gov

(Dated: July 16, 2009)

Abstract

We present a search for the lightest supersymmetric partner of the top quark in proton-antiproton collisions at a center-of-mass energy $\sqrt{s} = 1.96$ TeV. This search was conducted within the framework of the R_p conserved Minimal Supersymmetric extension of the Standard Model, assuming the decay $\tilde{t} \to l^+ + \tilde{\nu}_l + b$ is dominant. We searched a total of $\mathcal{L} = 1$ fb^{-1} of data collected by the CDF experiment requiring two leptons of opposite electric charge, at least one jet, and missing transverse energy. No significant evidence of the stop signal was found. Exclusion limits at 95% confidence level in the stop versus sneutrino mass plane are set.

Preliminary Results for Summer 2009 Conferences

1 Introduction

The Minimal Supersymmetric Standard Model[1] (MSSM) was introduced to provide possible explanations for several problems that arise in the Standard Model (SM). These include the hierarchy problem that requires fine tuning of theoretical parameters in order to avoid large quantum corrections and also the convergence of the strong, weak, and electromagnetic gauge couplings at the GUT scale.

MSSM assigns a new bosonic counterpart to each SM fermion and likewise a fermionic superpartner to each SM boson. The mass eigenstates of these supersymmetric quarks (squarks) can be a mixture of their weak eigenstates. The large mass of the top quark can then lead to a large splitting between the two mass eigenstates of the stop quark (stop). In fact the lighter of the two stops may be the lightest of all the squarks with a mass even below the top quark. That would make its detection at the Tevatron a realistic possibility.

In R-parity conserved MSSM, stop quarks are produced in pairs. Feynman diagrams for the dominant stop production processes at the Tevatron are shown in Figure 1

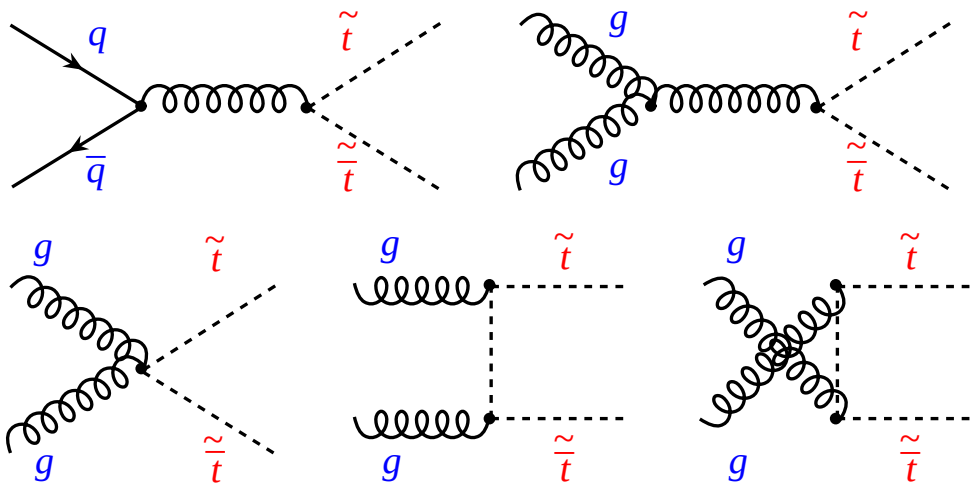

Figure 1: Feynman diagrams for stop quark production at the Tevatron

The stop quarks can decay via several possible channels depending on the masses of the particles involved. Two body decays such as :

$$\tilde{t} \to t\tilde{\chi}_1^0$$
$$\tilde{t} \to b\tilde{\chi}_1^+$$
$$\tilde{t} \to c\tilde{\chi}_1^0$$

may not be kinematically possible for a light stop or may be unlikely on account of LEP results [2]. This leaves three body decays like :

$$\tilde{t} \rightarrow W^+ b \tilde{\chi}_1^0$$
$$\tilde{t} \rightarrow b \tilde{l^+} \nu_l$$
$$\tilde{t} \rightarrow b l^+ \tilde{\nu_l}$$

Again limits from LEP on the slepton and neutralino masses disfavor the first two decays. This leaves the decay

$$\tilde{t} \rightarrow b l^+ \tilde{\nu_l}$$

which is the subject of this analysis. We assume the branching ratio for this decay mode is 100% and that lepton universality holds so that electrons, muons, and taus are equally likely decay products. While electrons and muons are detected directly, taus are only included opportunistically through their decays into electrons and muons. We also assume that the neutralino is the lightest stable particle (LSP) or decays neutrally into the LSP, thus escaping undetected and leading to missing transverse energy ($\not\!\!E_T$). Since stops are produced in pairs, the signature we look for is two opposite-sign leptons, missing transverse energy, and at least one jet.

2 Data Sample

The data sample consists of a dilepton data set with integrated luminosity of $0.97 fb^{-1}$ collected using the CDF II detector at Fermilab studying $p\bar{p}$ collisions at a center-of-mass energy $\sqrt{s} = 1.96$ TeV. Of particular relevance to this analysis are the tracking system, the calorimetry, and the muon detectors. The tracking system consists of silicon micro-strip detectors, the Silicon Vertex Detector (SVX) and the Intermediate Silicon Layers (ISL), which cover the pseudorapidity region $\mid \eta \mid < 2$ and a multi-wire open-cell drift chamber, the Central Outer Tracker (COT), with coverage in pseudorapidity of $\mid \eta \mid < 1$. The tracking system is surrounded by a superconducting solendoid with a magnetic field of 1.4 T. Outside the magnet are electromagnetic and hadronic calorimeters arranged in a projective tower geometry. This analysis uses the Central Electromagnetic Calorimeter (CEM) and the Central Hadronic Calorimeter (CHA). The CEM utilizes lead-scintillator sampling and covers $\mid \eta \mid < 1.1$ while the CHA uses iron-scintillator sampling and covers $\mid \eta \mid < 1.3$. Additional calorimetry extends the coverage to $\mid \eta \mid < 3.6$ and is used in calculating missing transverse energy and finding jets but not for lepton identification. Outside the calorimetry is the muon detection system. The parts of the muon detector relevant to this analyis are the Central Muon Detector (CMU), the Central Muon Upgrade Detector (CMP) and the Central Muon Extension (CMX). CMU consists of four layer drift chambers and covers the pseudorapidity range $\mid \eta \mid < 0.6$. CMP is made of four layers of single-wire drift cells located behind an additional 3.3 interaction lengths of steel and covers $\mid \eta \mid < 0.5$. Muon stubs found in both CMU and CMP are labelled CMUP muons. CMX extends the coverage to $\mid \eta \mid < 1$ and is made up of eight layers of drift tubes.

The data were collected using a three level trigger system. The events used in this analysis are required to contain at least two leptons falling into one of the following categories: CEM-CEM, CEM-CMUP, CEM-CMX, CMUP-CMUP, and CMUP-CMX where the leptons are labelled by the detector component used in their identification. Note that CMX-CMX muons are not included.

3 Background Determination

Several background sources can contribute to events with dileptons, jets, and missing transverse energy. These backgrounds are :

- $t\bar{t}$
- Heavy flavor production ($b\bar{b}$, $c\bar{c}$)
- Drell-Yan production of lepton pairs plus jets
- WW, WZ, ZZ, and Wγ production (dibosons)
- misidentified leptons

The $t\bar{t}$, Drell-Yan, and diboson backgrounds were estimated by generating Monte Carlo events using PYTHIA [3] followed by a run-dependent detector simulation. The background due to "misidentified" leptons consists of hadrons misidentified as leptons and uninteresting leptons from decays-in-flight of pions and kaons. To estimate this background a "fake rate" was first determined from samples of jet events in which a negligible number of real leptons relevant to this analysis are expected. The electron fake rate is defined as the ratio of the number of candidates passing electron ID cuts to the number of central jets with $E_T > 4$ GeV. For muons the fake rate is the ratio of candidates passing muon ID cuts to the number of isolated tracks passing track quality cuts. The fake rates were determined as a function of jet E_T for electrons and track p_T for muons. These fake rates are then applied to each "fakeable" jet or track, one object at a time, in a sample of single lepton events taken with the 8 GeV/c electron calibration trigger and the 8 GeV/c muon calibration trigger. Events with a single trigger lepton and a second "fake" lepton that pass the analysis cuts are assigned an appropriate weight and form the misidentified lepton background sample. The systematic uncertainty on the misidentifed lepton background is conservatively set at 50%.

The background arising from heavy flavor ($b\bar{b}$, $c\bar{c}$) production was also estimated using actual data. A data sample enriched in heavy flavor events was selected by inverting the normal impact parameter (d_0) cuts. Specifically it was required that $| d_0 | > 0.2$ cm for COT only tracks and $| d_0 | > 0.02$ cm if SVX information was available. The only significant contributions to this heavy flavor enriched data sample are Drell-Yan, heavy flavor, and misidentified leptons. The Drell-Yan contribution was derived from Monte Carlo samples and the misidentified lepton component was estimated

using the technique described above. The remaining events were attributed to heavy flavor and used to determine the shape of the heavy flavor dilepton mass distribution. Scaling factors were determined by fitting the dilepton invariant mass distributions in the range $15 < M_{ll} < 35$ GeV/c^2 and letting the heavy flavor normalization float. The resulting scaling factors were then applied to "inverse d_0" events in various control regions as well as the signal region to estimate the heavy flavor background. It should be noted that no heavy flavor contribution to the signal region survives our final cuts.

A total of 74 Monte Carlo signal samples were generated using PYTHIA and run through full detector simulation. The events were scaled to the next-to-leading order Prospino cross-section [4, 5] with the CTEQ6M parton distribution function. Various stop and sneutrino masses were generated with the stop mass ranging from 55 to 190 GeV/c^2 and the sneutrino mass from 45 to 110 GeV/c^2.

4 Event Selection

At the preliminary analysis stage the following cuts are applied to improve the data quality:

- The reconstructed event Z-vertex $|Z_{vtx}| < 60$ cm
- Cosmic ray and beam halo events are rejected using timing and tracking information
- Electron and muon candidates are required to pass standard ID cuts. Scale factors are applied to account for differences in lepton ID efficiency between data and Monte Carlo. Electrons are required to be more than 0.5 degrees away from a calorimeter boundary in phi.
- Jets are identified using a cone-based algorithm with a cone size $R = 0.7$. η-dependent corrections are applied to make the calorimeter response to jet energies uniform in η. Additional corrections are applied to account for multiple $p\bar{p}$ interactions and for energy loss in uninstrumented portions of the detector or any non-linearity in calorimeter response.
- Missing transverse energy ($\not\!\!E_T$) is calculated from energy deposition in the calorimeters. Corrections are applied for the two highest p_T leptons in the event. Since muons are minimum ionizing particles and deposit typically only 2 GeV in the calorimeters, $\not\!\!E_T$ is corrected using p_T from tracking. Any correction to electron E_T is also incorporated as a $\not\!\!E_T$ correction. $\not\!\!E_T$ is also adjusted to account for the jet energy corrections described above. All jets with corrected $E_T > 10$ GeV and $|\eta| < 2.4$ are included in the $\not\!\!E_T$ correction.

5 Systematic Uncertainties

Systematic errors from the following sources are included :

- Jet Energy Scale : The systematic uncertainty on the Jet Energy Scale was determined by varying the uncertainties on the contributions to the jet energy corrections up and down by one sigma. The resulting uncertainty varies from less than 1% to 35% and is largest for Drell-Yan events which typically have soft jets.
- Luminosity : The integrated luminosity is measured with a systematic uncertainty of 6%.
- Trigger Efficiency Uncertainty : The uncertainty on the dilepton trigger efficiency is estimated to be 2%.
- Lepton Identification: The uncertainty on electron and muon identification is determined to be 2%.
- Misidentified Leptons: The uncertainty on the background arising from misidentified electrons and muons is taken to be 50%.
- Parton Distribution Function: The uncertainty on the acceptance arising from the PDFs used in the Monte Carlo is estimated to be 2%.
- ISR/FSR : The uncertainty arising from Initial and Final State Radiation was determined by varying their contribution in the Monte Carlo. The resulting uncertainty varied from about 2% to 4% depending on the lepton flavors.
- Theoretical Cross-sections: The uncertainties on the theoretical cross-sections for the various background are listed below :
  - $t\bar{t}$ 8%
  - Drell-Yan 2%
  - WW 6%
  - WZ 8%
  - ZZ 10%
  - Wγ 7%

6 Control Regions

To check the accuracy of our estimation of Standard Model backgrounds, a number of control regions are defined as shown in Figure 2. dphi is the difference in azimuthal angle phi (ϕ) between the two leading leptons.

We require the leading lepton to have $p_T > 10$ GeV/c and the second lepton $p_T > 5$ GeV/c. Also the invariant mass of the two leading leptons must be greater than 15 GeV/c^2. The two leptons must be separated by

$$R = \sqrt{(\Delta\eta)^2 + (\Delta\phi)^2} > 0.4$$

Control Region A (not shown) consists of ee and $\mu\mu$ events with invariant mass $76 < M_{ll} < 106$ GeV/c^2. For ee the number of observed events is 12461 compared to a background expectation of 12335±63±923 where the first uncertainty is statistical and the second systematic. For $\mu\mu$ 7111 events were observed and 6946±43±550 were expected. Data agree well with background estimations. These "Z" events were excluded from other control regions as well as the pre-signal region.

Additional control regions were characterized by either low $\not\!\!E_T$ (< 15 GeV) or no jets with $E_T > 15$ GeV. Two of the control regions are characterized by low $\not\!\!E_T$ and at least one jet (B1 and C1). Control region B1 contains back-to-back leptons and Control region C1 the rest. The major source of events in the ee and $\mu\mu$ channels is Drell-Yan whereas in the $e\mu$ channel heavy flavor production is the major contribution. The data agree with background expectations for Control Regions B1 and C1. The remaining control regions contain no jets above 15 GeV with Control Regions D and E being particularly interesting since they have large $\not\!\!E_T$. Again the data are found to agree reasonably well (within two standard deviations) with background estimates.

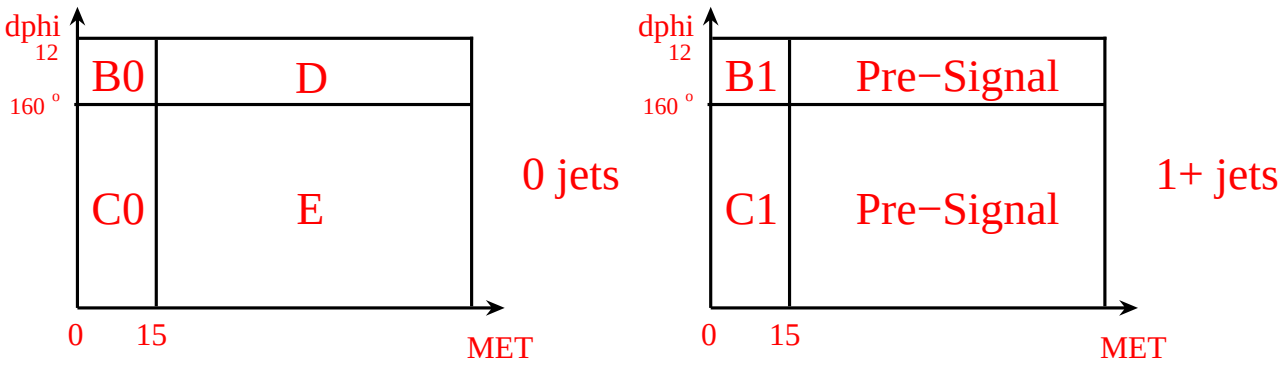

Figure 2: Definition of Control Regions.

	ee	$e\mu$	$\mu\mu$	*All*
DY	72.8±4.8±26.3	26.6±2.7±5.4	62.4±4.1±28.4	161.8±6.8±59.8
$t\bar{t}$	6.1±0.1±0.7	13.1±0.1±1.4	4.2±0.1±0.5	23.4±0.2±2.5
di-boson	3.5±0.1±0.6	6.2±0.1±1.1	2.1±0.0±0.4	11.8±0.1±2.0
l+fake	21.6±0.2±10.8	24.9±0.4±12.4	5.4±0.2±2.7	51.9±0.5±21.3
HF	9.1±4.1±7.4	30.6±7.9±10.5	8.5±4.3±6.7	48.1±9.9±14.5
Exp.Bkg.	113.1±6.3±29.8	101.4±8.4±17.6	82.6±5.9±29.6	297.0±12.0±66.3
Obs.	110	76	89	275

Table 1: Expected backgrounds and observed events for the pre-signal region

7 Pre-signal Region

We define a pre-signal region by applying several cuts to improve the data quality and to provide a data sample loosely consistent with the SUSY signature for which we are searching. Later final cuts will be applied to this sample that minimize the 95% confidence level upper limit on the production cross-section for stop. At the pre-signal stage the following cuts are applied :

- Two opposite sign leptons must be present with the highest p_T lepton having $p_T > 10$ GeV/c and the second highest lepton $p_T > 5$ GeV/c.
- The invariant mass of the two leading leptons must be greater than 15 GeV/c^2.
- We require at least one jet with corrected $E_T > 15$ GeV and $|\eta| < 2.0$.
- $\not\!\!E_T > 15$ GeV is required.
- Several isolation cuts are imposed. If one of the two highest p_T leptons is an electron and
$$R = \sqrt{(\Delta\eta)^2 + (\Delta\phi)^2}$$
is less than 0.4 between the electron and the leading jet, the event is rejected. Likewise it is required that R > 0.4 between the two leptons. Finally we require $\Delta\phi > 20$ degrees between $\not\!\!E_T$ and each of the leading leptons and the leading jet.

Figure 3 gives the $\not\!\!E_T$ distributions separately for *ee*, $e\mu$ and $\mu\mu$ events as well as the summed distribution for the pre-signal region. The expected $\not\!\!E_T$ distribution for MC stop events with stop mass 150 GeV/c^2 and sneutrino mass 75 GeV/c^2 is also shown. Table 1 lists the sources of expected background for the pre-signal region and the actual number of observed events. Good agreement of data with background predictions is observed.

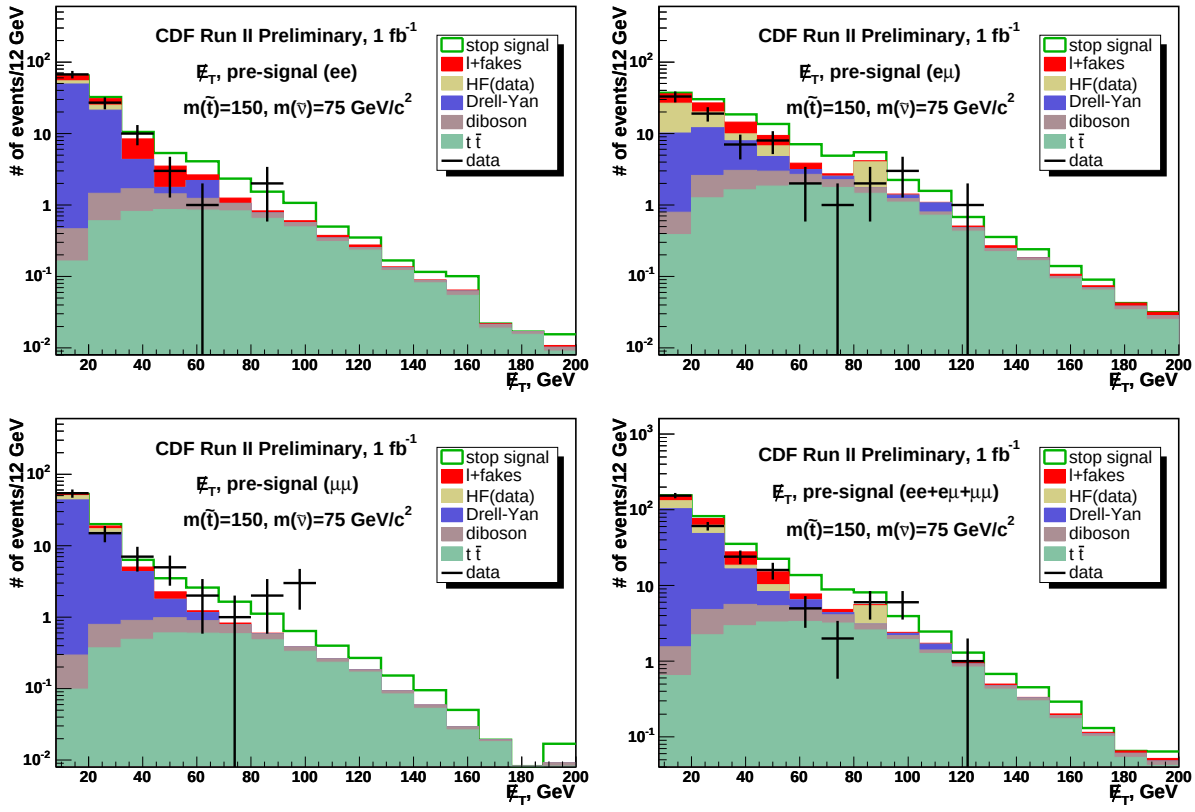

Figure 3: MeT plots for the Pre-Signal Region.

8 Analysis

We use the program Corlim[9] (with Bayesian statistics) to find the expected 95% confidence level upper limits on the Stop cross section for the 74 Stop-Snu points generated using the Pythia MC program. Choice of and starting values for the cuts used were found by maximizing Signal/$\sqrt{Bkg}$. Corlim is then used for tuning one variable at a time with the remaining variables fixed at their optimal values and iterating as needed.

The variables used to discriminate MC stop signal from background are :

- Missing transverse energy ($\not{E}_T$)
- The difference in phi angle between the dilepton system and $\not{E}_T$
- $H_T = \not{E}_T + p_{T1} + p_{T2} + E_{Tj}$ where p_{T1} is the transverse momentum of the leading lepton, p_{T2} is the transverse momentum of the second leading lepton, and E_{Tj} is the transverse energy of the leading jet
- The transverse momentum of the second leading lepton
- The transverse momentum of the dilepton system
- The transverse mass between each lepton and $\not{E}_T$ where

$$M_T = \sqrt{2p_T * \not{E}_T \ * (1 - cos(\Delta\phi(lepton - \not{E}_T\ )))}$$

The optimum values for the cut variables depend predominantly on the $\Delta M = M_{\tilde{t}} - M_{\tilde{\nu}}$ mass difference and can be grouped into four sets labeled a through d in bands parallel to the $M_{\tilde{t}} = M_{\tilde{\nu}} + M_b$ kinematic limit. The values used for the cuts in each of the cut groupings are given in Table 2.

With the exception of the uncertainty on the theoretical Stop cross-section, all uncertainties, both uncorrelated and correlated, are incorporated into the upper limit determinations which are then compared to the theoretical Stop cross-section. Stop-Snu points whose cross-sectional upper limits are less than the theoretical cross-section are considered excluded at the 95% confidence level.

Variables	Cut groups			
$\Delta M = M_{\tilde{t}} - M_{\tilde{\nu}}$, GeV/$c^2$	$5 < a <$ 47.5	$< b <$ 72.5	$< c <$ 87.5	$< d$
$\not\!\!E_T >$	25 GeV	32 GeV	32 GeV	32 GeV
$d\phi$(dilep-$\not\!\!E_T$)>	60°	60°	60°	60°
$p_{T2} >$	7 GeV/c	7 GeV/c	7 GeV/c	7 GeV/c
H_T min	—	>120 GeV	>130 GeV	>165 GeV
H_T max	<170 GeV	<225 GeV	<290 GeV	—
M_T (lep,$\not\!\!E_T$)>	15 GeV	11 GeV	—	—
p_T (dilep)<	Sliding Cut	—	—	—

Table 2: Table of cuts for different groups.
lep = both leptons, dilep = dilepton system, 2 = second (lower p_T) lepton. The sliding cut is determined by a linear fit to the optimal dilepton p_T value as a function of ΔM in cut group a. (Cut = 0.98*ΔM - 1.03)

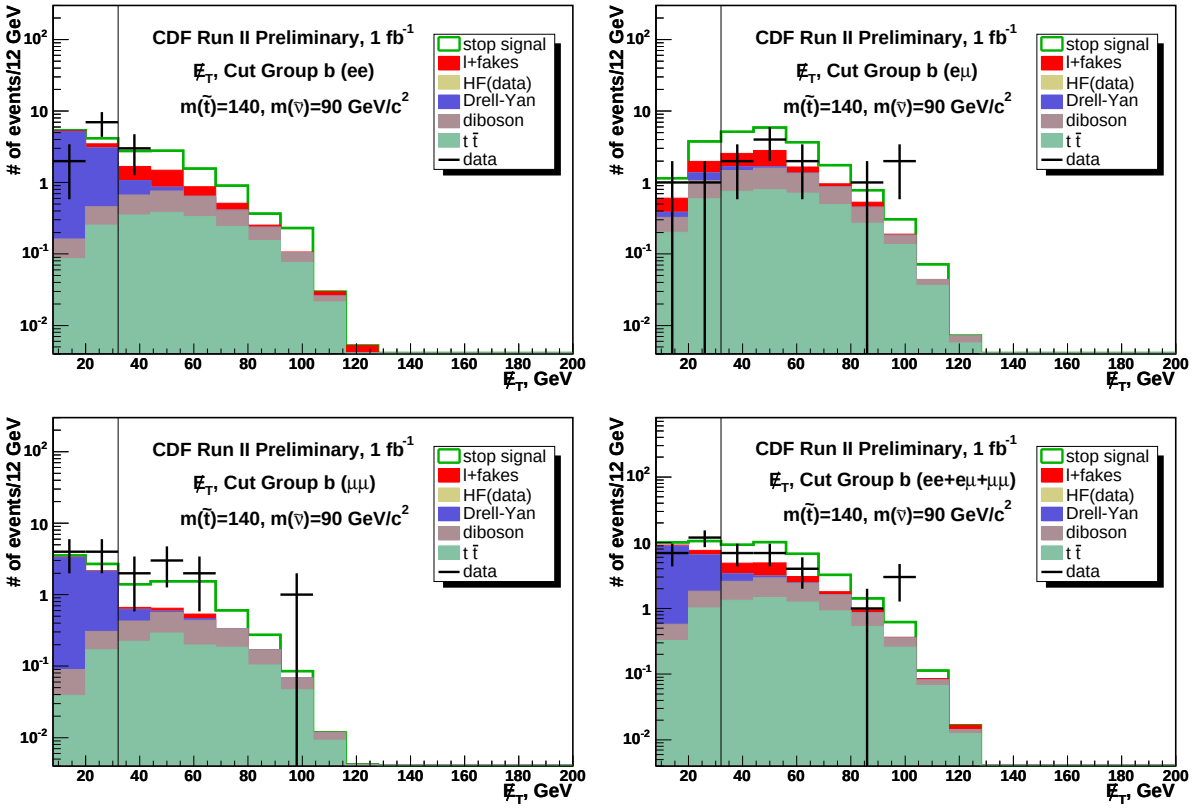

Figure 4: (N-1) MeT plots for cut group b.

9 Results

The $\not\!\!E_T$ distributions for the signal region is shown in Figure 4 for cut group b. The individual backgrounds are shown as well as the data. For reference the expected signal from the stop-sneutrino point (140,90) is also shown. The vertical line represents the cut placed on $\not\!\!E_T$ for cut group b. In general the agreement between data and Standard Model background is quite good although the statistics are low. The exception is an excess of data over background expectatations for $\mu\mu$ events at large $\not\!\!E_T$. This is quantified in Tables 3 through 6. These results are not independent observations since there is a large overlap in events between cut groups b, c, and d. The largest muon excess, found in cut group b, does not rise to the level of three standard deviation significance.

	ee	$e\mu$	$\mu\mu$	All
DY	0.86±0.19±0.31	0.32±0.10±0.06	0.56±0.15±0.26	1.8±0.3±0.6
$t\bar{t}$	0.13±0.01±0.01	0.28±0.02±0.03	0.06±0.01±0.01	0.5±0.0±0.1
diboson	0.52±0.02±0.09	0.96±0.03±0.16	0.28±0.01±0.05	1.8±0.0±0.3
l+fake	1.74±0.04±0.87	2.01±0.09±1.00	0.18±0.03±0.09	3.9±0.1±1.7
Exp. Bkg.	3.25±0.20±0.93	3.57±0.14±1.01	1.08±0.15±0.28	7.9±0.3±1.9
$\tilde{t}\bar{\tilde{t}}$(130/95)	3.25±0.32±0.36	6.64±0.43±0.68	2.92±0.27±0.32	12.8±0.6±1.3
Obs.	1	2	1	4

Table 3: Cut group a results for (130/95).

	ee	$e\mu$	$\mu\mu$	All
DY	0.49±0.15±0.18	0.28±0.09±0.06	0.25±0.10±0.11	1.0±0.2±0.4
$t\bar{t}$	1.57±0.05±0.17	3.20±0.07±0.34	1.06±0.04±0.12	5.8±0.1±0.6
diboson	1.28±0.02±0.21	2.75±0.03±0.47	0.96±0.01±0.17	5.0±0.0±0.9
l+fake	1.59±0.03±0.80	2.50±0.12±1.25	0.16±0.04±0.08	4.3±0.1±1.8
Exp. Bkg.	4.93±0.15±0.86	8.73±0.17±1.38	2.43±0.12±0.25	16.1±0.3±2.3
$\tilde{t}\bar{\tilde{t}}$(140/90)	3.71±0.29±0.33	8.85±0.42±0.72	3.02±0.23±0.28	15.6±0.6±1.3
Obs.	3	11	8	22

Table 4: Cut group b results.

	ee	$e\mu$	$\mu\mu$	All
DY	0.78±0.18±0.28	0.33±0.09±0.07	0.37±0.11±0.17	1.5±0.2±0.5
$t\bar{t}$	3.28±0.07±0.36	7.11±0.10±0.75	2.31±0.06±0.26	12.7±0.1±1.4
diboson	1.36±0.02±0.23	2.93±0.03±0.50	1.00±0.01±0.18	5.3±0.0±0.9
l+fake	1.25±0.03±0.62	2.10±0.12±1.05	0.24±0.08±0.12	3.6±0.1±1.5
Exp. Bkg.	6.67±0.20±0.80	12.47±0.18±1.39	3.92±0.15±0.38	23.1±0.3±2.6
$\tilde{t}\bar{\tilde{t}}$(150/75)	6.08±0.24±0.46	12.6±0.3±0.9	4.21±0.18±0.34	22.9±0.4±1.6
Obs.	7	13	9	29

Table 5: Cut group c results.

	ee	$e\mu$	$\mu\mu$	All
DY	0.37±0.13±0.13	0.06±0.04±0.01	0.52±0.14±0.24	1.0±0.2±0.4
$t\bar{t}$	4.37±0.08±0.48	9.37±0.12±0.99	3.04±0.06±0.35	16.8±0.2±1.8
diboson	0.89±0.01±0.15	1.93±0.02±0.33	0.67±0.01±0.12	3.5±0.0±0.6
l+fake	0.61±0.02±0.30	1.36±0.16±0.68	0.15±0.07±0.08	2.1±0.2±0.9
Exp. Bkg.	6.24±0.15±0.60	12.72±0.20±1.25	4.38±0.17±0.45	23.3±0.3±2.4
$\tilde{t}\bar{\tilde{t}}(180/50)$	3.45±0.12±0.24	7.26±0.16±0.49	2.34±0.09±0.18	13.0±0.2±0.9
Obs.	5	11	8	24

Table 6: Cut group d results.

We proceed to set 95% confidence level upper limits on the production cross section for each point in the stop-sneutrino mass plane, using the program Corlim with Bayesian statistics and using the three dilepton flavor channels jointly with full treatment of correlated and uncorrelated errors between them. This is a blind analysis and the analysis cuts and procedures were established without knowledge of the data in the signal regions. It should be noted, however, that the cleanup cut requiring the difference in azimuthal angle between $\not\!\!E_T$ and each of the two leading leptons and the leading jet be greater than 20° was introduced after the first 310 pb^{-1} of data had been examined.

One-dimensional curves of the upper cross-section limits vs the theoretical cross-section are shown in Figure 5 for groups of points with fixed stop-sneutrino mass differences. It is seen that the cross section upper limits for a given ΔM tend to be rather independent of stop mass.

We determine the expected exclusion contour shown in Figure 6 by comparing the cross-section limits obtained by setting the number of observed events equal to the expected Standard Model background with the central value of the theoretical NLO Prospino stop cross-section. We interpolate linearly between nearby excluded and not-excluded points. Similarly we obtain the observed exclusion contour by comparing the cross-section limits obtained from the number of events found in the data with the theoretical cross-section. This is shown in Figure 7 along with previously existing limits [7, 8]. This analysis extends the world exclusion limits to higher sneutrino masses for stop masses in the range from 135 to 155 GeV/c^2 and to higher stop masses, up to 180 GeV/c^2, for low sneutrino masses.

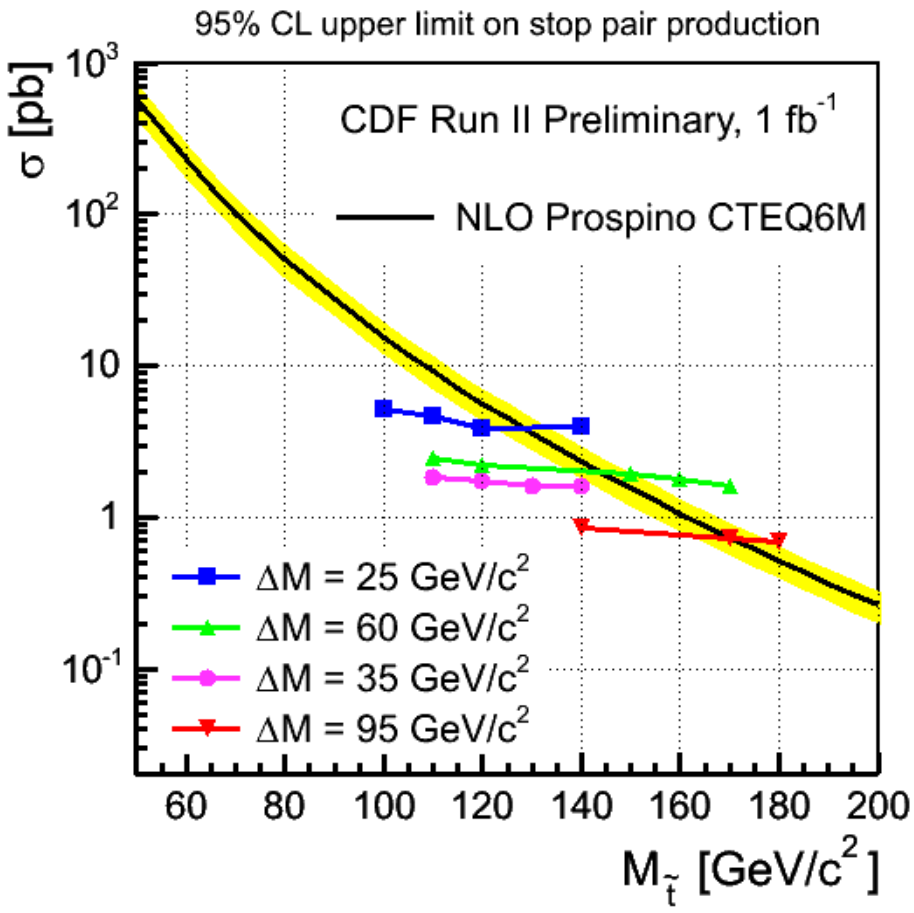

Figure 5: Limit plot.

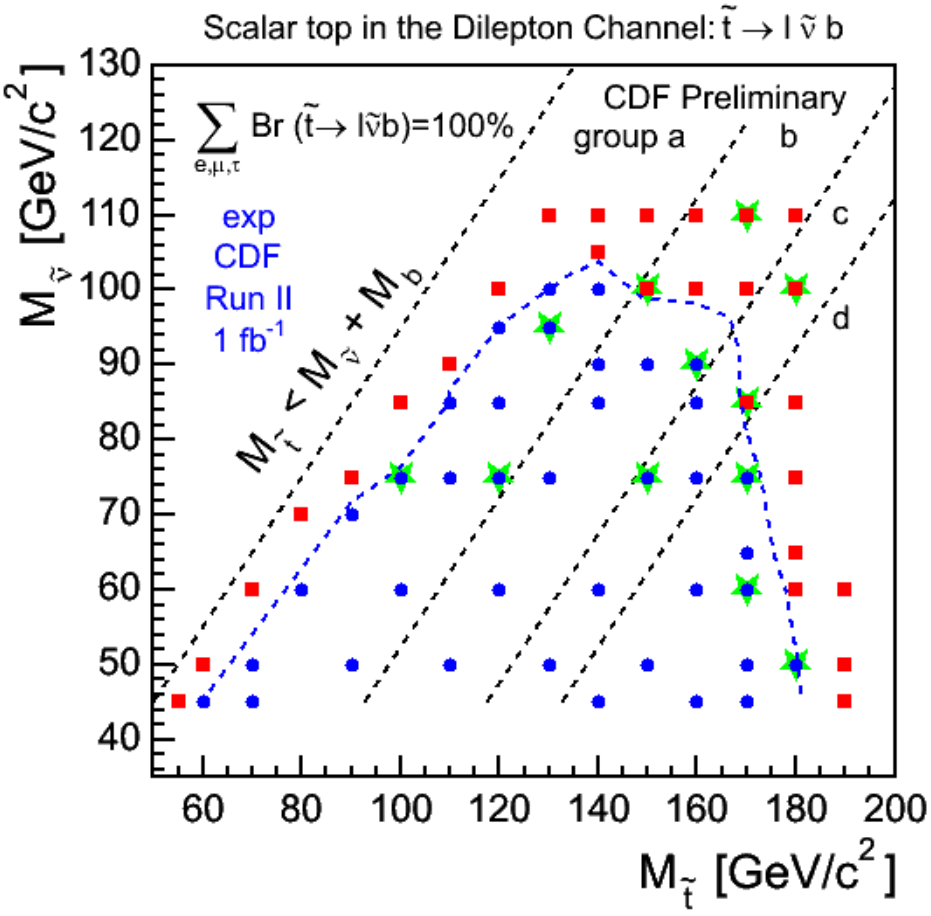

Figure 6: Contour plot of the expected limit in the stop-sneutrino plane showing the individual stop-sneutrino points. Blue dots are excluded, red squares are not excluded, and green stars denote points used for tuning cuts.

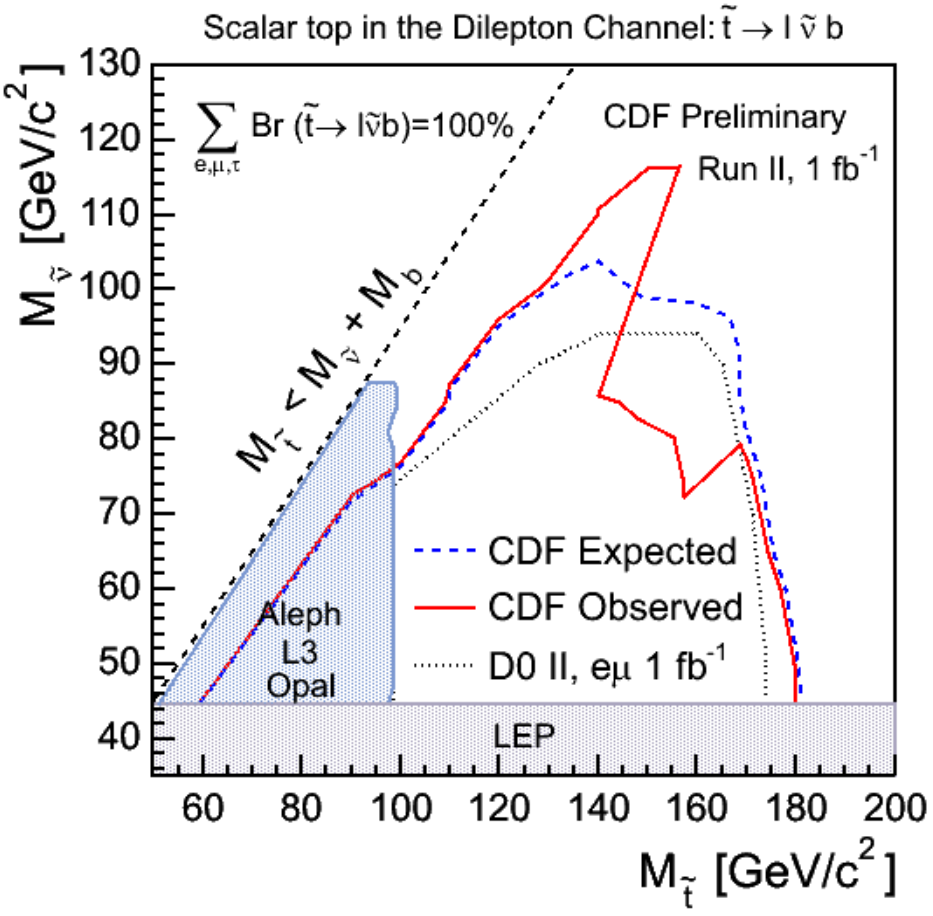

Figure 7: Observed/expected limits in the stop-sneutrino plane.

10 Acknowledgments

We thank the Fermilab staff and the technical staffs of the participating institutions for their vital contributions. This work was supported by the U.S. Department of Energy and National Science Foundation; the Italian Istituto Nazionale di Fisica Nucleare; the Ministry of Education, Culture, Sports, Science and Technology of Japan; the Natural Sciences and Engineering Research Council of Canada; the National Science Council of the Republic of China; the Swiss National Science Foundation; the A.P. Sloan Foundation; the Bundesministerium für Bildung und Forschung, Germany; the Korean Science and Engineering Foundation and the Korean Research Foundation; the Science and Technology Facilities Council and the Royal Society, UK; the Institut National de Physique Nucleaire et Physique des Particules/CNRS; the Russian Foundation for Basic Research; the Ministerio de Ciencia e Innovación, and Programa Consolider-Ingenio 2010, Spain; the Slovak R&D Agency; and the Academy of Finland.

References

[1] S. Dimopoulos and H. Georgi, Nucl. Phys. B **193**, 150 (1981).

[2] LEP SUSY Working Group ALEPH DELPHI L3 and OPAL Collaborations. LEPSUSYWG/01-03.1,http:lepsusy.web.cern.ch/lepsusy/, 2001; LEPSUSYWG/02-01.1,http:lepsusy.web.cern.ch/lepsusy/, 2002; LEPSUSYWG/02-02.1,http:lepsusy.web.cern.ch/lepsusy/, 2002.

[3] T.Sjöstrand, L.Lönnblad and S.Mrenna, JHEP **0612** 046 (2005).

[4] W.Beenakker, M.Hopker, M.Spira, and P.Zerwas, Nucl. Phys. **B** 51 (1997).

[5] W.Beenakker, M.Hopker, and M.Spira, Nucl. Phys. hep-ph/9611232 (1996).

[6] W.Beenakker, R.Höpker and M.Spira, " PROSPINO: A Program for the Production of Supersymmetric Particles in Next-to-leading Order QCD" , hep-ph/9611232.

[7] CDF Collaboration, Phys. Rev Let. **90** 251801 (2003).

[8] V.M.Abazov et al, The D0 Collaboration, Phys. Lett **B** 675, 289 (2009).

[9] John Conway, CDF internal note 6428.